Reactions of Laser-Ablated Al, Ga, In, and Tl Atoms with Hydrogen Cyanide in Excess Argon. Matrix Infrared Spectra and Density Functional Theory Calculations on New Cyanide and Isocyanide Products

Dominick V. Lanzisera and Lester Andrews*

Department of Chemistry, University of Virginia, Charlottesville, Virginia 22901

Received: July 17, 1997; In Final Form: October 10, 1997[⊗]

Laser-ablated Al, Ga, In, and Tl atoms react with hydrogen cyanide in the presence of excess argon to produce matrix-isolated linear cyanides and isocyanides, MCN and MNC, respectively. Similar to the products of alkaline earth reactions with hydrogen cyanide and unlike the corresponding boron reactions, no products containing hydrogen are formed. Experiments with $H^{13}CN$ generate $MN^{13}C$ shifted 40 cm^{-1} from $MN^{12}C$ in the C≡N stretching mode, and this isotopic shift is virtually independent of the group 13 element. Similarly, the MCN molecules exhibit a carbon-13 shift of 45 cm^{-1}, with the isotopic shift approximately the same for each metal. As the mass of M increases, the C≡N frequency decreases for MCN and remains nearly constant for MNC. Group 13 reactions with HCN produce significant amounts of MCN, in contrast to the corresponding alkaline earth reactions. For aluminum, this disparity suggests that an insertion mechanism plays at least a partial role in product formation. For the heavier elements, photolysis behavior indicates that attack on the nitrogen atom is dominant, with MCN produced following rearrangement of MNC.

Introduction

Recent laser ablation matrix isolation studies on reactions of boron have uncovered several new boron products.[1−4] In one of these studies, involving boron and hydrogen cyanide, five new major products were formed: BNC, BCN, HBNC, HBCN, and cyclic HB(CN).[4] The first two products dominate the spectra, exhibiting strong C≡N stretching absorptions. Analogous experiments have been performed for group 2 metals with HCN; although Be gave similar products to B, the heavier group 2 metals produced only MNC compounds.[5,6]

Elements in group 13 of the periodic table (formerly group IIIB) are characterized by three valence electrons. As a result, fulfilling the octet in covalent bonding requires donation of electrons from another atom to an empty orbital of the group 13 atom, making compounds of these elements strong Lewis acids.[7] This trait is strongest for boron and becomes less of a factor as the size of the group 13 element increases. For example, because the octet is not filled, BH_3 does not exist as a stable borane at room temperature, instead dimerizing to B_2H_6. In recent matrix reactions of boron and aluminum with ammonia, different major products were formed.[8−10] The additional filled shell in the electron core of aluminum affects its chemistry in a profound way.

There has been recent interest in the characteristics of the AlCN and AlNC molecules. The carbon star IRC + 10216 typically ejects several molecules containing carbon, including MgNC.[11] Because the metal halides, AlCl and AlF, have also been observed,[12] Schaefer and co-workers[13] have calculated the spectroscopic constants and energetics of AlCN and AlNC. According to their results, AlNC is the more stable isomer by 5.5 kcal mol^{-1}, and there is a 6 kcal mol^{-1} activation energy for the isomerization of AlCN to AlNC.

This article presents matrix isolation studies of reactions of Al, Ga, In, and Tl with HCN. Infrared spectra show the absorptions for the major products, and DFT calculations aid in the identification of these products. In the study of Be with HCN, the BP86 functional proved very effective at predicting the matrix frequencies and is used here to help identify the products. In addition to these calculated absorption frequencies, the relative energies and geometries of these products provide insight into the nature of MCN and MNC molecules, where M is the group 13 atom.

Experimental Section

The apparatus and procedure for pulsed-laser ablation, matrix isolation, and FTIR spectroscopy have been described previously.[1−6,8−10] Mixtures of 0.3% HCN or $H^{13}CN$ in Ar were co-deposited at 3 mmol/h for 2 h onto a 6−10 K cesium iodide window and reacted with metal atoms ablated from a solid target source rotating at 1 rpm. The fundamental 1064 nm beam of a Nd:YAG laser (Spectra Physics DCR-11) operating at 10 Hz and focused with a focal length = +10 cm lens ablated the target using 10−30 mJ per 10 ns pulse. The samples employed were Al (Aesar, 99.998% Puratronic), Ga (Aesar, 99.99999%), In (Indium Corp. of America, 99.99%), and Tl (Spex, 99.999%). The gallium target rod was cooled by an ice bath in thermal contact with the rod outside of the reaction cell. The procedures for preparing HCN and $H^{13}CN$ have been described previously.[4,6,11]

Density functional theory (DFT) calculations were performed on potential product molecules using the Gaussian 94 program package.[15] These calculations used the BP86 pure DFT functional[16,17] with effective core potentials for the M atoms. The basis sets for the light atoms were 6-311G with one single first polarization function (6-311G*),[18,19] and the LANL2DZ basis sets[20−22] were used for the group 13 atoms. More sophisticated basis sets would not work for TlCN and TlNC calculations, and the same method was employed for the all molecules for the sake of comparison.

Results

Matrix infrared spectra in the C≡N stretching region for the products of M + HCN (M = Al, Ga, In, Tl) reactions are reported for both ^{12}C and ^{13}C reagents. All pertinent peak

[⊗] Abstract published in *Advance ACS Abstracts,* November 15, 1997.

S1089-5639(97)02333-5 CCC: $14.00

TABLE 1: Observed Frequencies (cm^{-1}) for Products from Reactions of Hydrogen Cyanide with Group 13 Elements

M + $H^{12}CN$	M + $H^{13}CN$	photolysis[a]	annealing[b]	identity
2306.9	2306.9	+10	−35	$(H_2)^{10}BH$
2298.3	2298.3	+10	−35	$(H_2)^{11}BH$
2268.3	2268.3	+40	+15	^{10}BH
2259.4	2259.4	+40	+15	^{11}BH
2171.5	2122.8	−30	−20	^{10}BCN
2170.7	2122.1	−30	−20	^{11}BCN
2068.0	2039.6	+30	−30	^{10}BNC
2055.2	2021.6	+30	−30	^{11}BNC
2143.7	2097.3	+5	−5	AlCN
2067.9	2028.3	−5	+10	AlNC site
2064.4	2024.7	+15	−65	AlNC site
2051.4	2011.2	+40	−40	AlNC
1590.9	1590.9	0	0	AlH
532.0	526.7	+40	−40	AlNC
456.2	450.3	+5	−5	AlCN
2137.8	2091.7	+25	−5	GaCN
2052.0	2009.3	+10	−25	GaNC site
2046.4	2005.8	−15	−15	GaNC
1513.8	1513.8	+10	+10	GaH
2132.4	2086.7	+110	0	InCN
2051.1	2009.9	−35	−15	InNC
1387.4	1387.4	0	0	InH
2125.7	2080.4	+30	0	TlCN
2051.9	2009.2	0	−20	TlNC site
2047.7	2006.4	−40	−10	TlNC
1309.3	1309.3	0	0	TlH
2154.0	2017.5			$(CN)_2$
2044.3	2002.0			CN
2027.8	1984.9			HNC
477.8	477.3			HNC

[a] Percent increase or decrease on broad-band photolysis for 30 min. [b] Percent increase or decrease on annealing to 25 K.

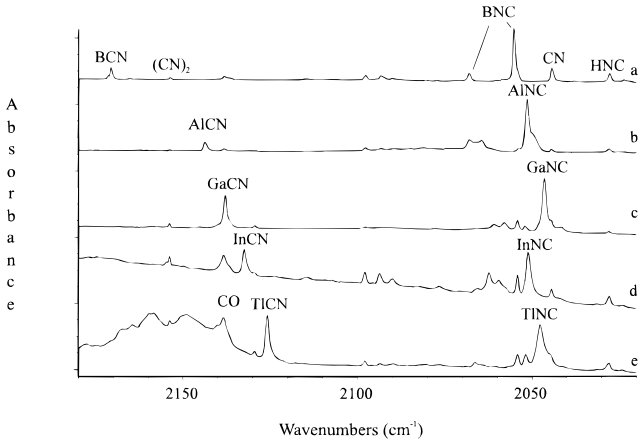

Figure 1. Matrix infrared spectra in the 2180−2020 cm^{-1} C≡N stretching region following pulsed laser ablation of alkaline earth metals co-deposited with Ar/$H^{12}CN$ (300/1) samples on a CsI window at 6−7 K: (a) B, (b) Al, (c) Ga, (d) In, and (e) Tl.

absorptions, including the metal monohydrides,[23−26] are listed in Table 1, along with their respective photolysis and annealing behaviors. Except for boron experiments,[4] reactions of group 13 atoms with DCN produced no cyanide products distinct from those in the HCN experiments, and these experiments will not be discussed here. Figures 1 and 2 compare the C≡N stretching regions for all products from $H^{12}CN$ and $H^{13}CN$, respectively. The spectra are not on common scale and are instead normalized to each other because the higher yield absorptions in the boron and aluminum experiments would dominate and obscure those of gallium, indium, and thallium. The higher yield of boron and aluminum experiments results from the relative hardness of these targets and the ability to ablate them at higher laser energy.

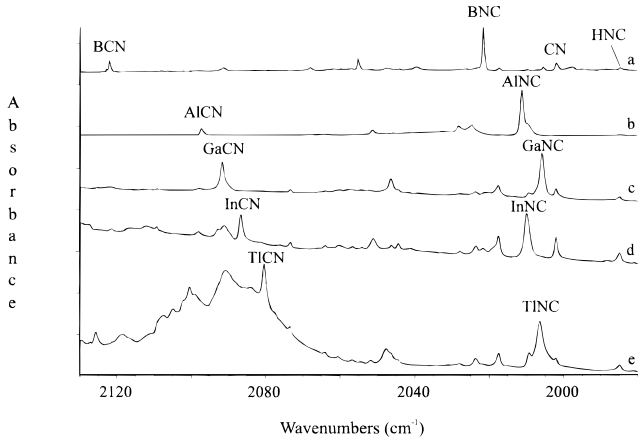

Figure 2. Matrix infrared spectra in the 2130−1980 cm^{-1} C≡N stretching region following pulsed laser ablation of alkaline earth metals co-deposited with Ar/$H^{13}CN$ (300/1) samples on a CsI window at 6−7 K: (a) B, (b) Al, (c) Ga, (d) In, and (e) Tl.

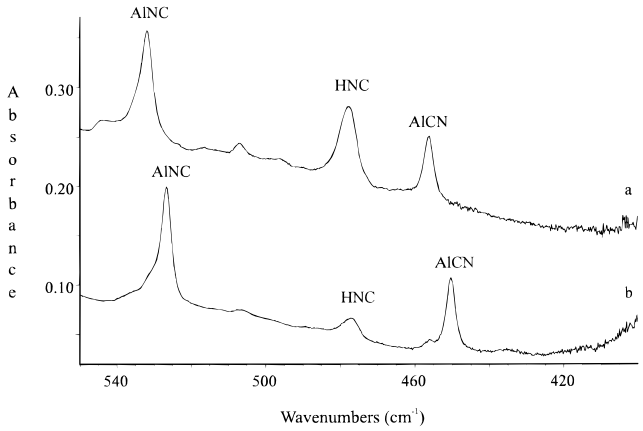

Figure 3. Matrix infrared spectra in the 550−400 cm^{-1} Al−N and Al−C stretching regions following pulsed laser ablation of Al atoms co-deposited with Ar/HCN (300/1) samples on a CsI window at 6−7 K: (a) Al + $H^{12}CN$ and (b) Al + $H^{13}CN$.

Al + HCN. Figure 1b illustrates the spectrum of Al and $H^{12}CN$ reaction products, while Figure 2b gives the spectrum from Al + $H^{13}CN$ reactions, following 2 h of deposition. In the $H^{12}CN$ experiment, the main band at 2051.4 cm^{-1} has a red shoulder that increases on photolysis, leading to the large increase in size noted in Table 1. Annealing the matrix reduces the intensity of this band substantially. The obvious $H^{13}CN$ counterpart, with similar photolysis and annealing behavior, appears at 2011.2 cm^{-1}, yielding a carbon-13 shift of 40.2 cm^{-1}. For both isotopic precursors, a weak doublet appears at approximately 15 cm^{-1} above the strongest band. One absorption, at 2064.4 and 2024.7 cm^{-1} for ^{12}C and ^{13}C, respectively, increases in intensity a small amount on photolysis before decreasing on annealing while the other absorption of this doublet is nearly unchanged on photolysis and annealing.

The final significant absorptions in Figures 1b and 2b appear at 2143.7 and 2097.3 cm^{-1}, respectively. These bands show a small increase on photolysis and small decrease on annealing and are shifted 46.4 cm^{-1} from each other, a shift somewhat larger than for the strongest bands at 2051.4 and 2011.2 cm^{-1}. In addition, AlH was observed at 1590.9 cm^{-1}.[23]

According to previous work,[10,27] Al−N and Al−C single bonds should be observable above 400 cm^{-1}, and Figure 3 presents a spectrum in the 550−400 cm^{-1} region. In addition to the HNC bands, two new pairs of absorptions are observed. The first of these, at 532.0 and 526.7 cm^{-1}, increases a great deal on photolysis and decreases markedly on annealing, thereby

TABLE 2: DFT/BP86 Calculations for MCN and MNC, Where M = B, Al, Ga, In, or Tl

product	energy (au)	bond lengths (Å)[a]	freq, cm^{-1} (int, km mol^{-1})[b]
BNC	−117.566 90	$r_{BN} = 1.46$; $r_{CN} = 1.20$	2010.5 (640), 884.2 (242), 62.3i (16 × 2)
BCN	−117.558 49	$r_{BC} = 1.61$; $r_{CN} = 1.17$	2177.2 (216), 743.5 (231), 103.0 (33 × 2)
AlNC	−94.858 46	$r_{AlN} = 1.94$; $r_{CN} = 1.19$	2024.4 (405), 491.2 (167), 71.6 (1 × 2)
AlCN	−94.853 86	$r_{AlC} = 2.09$; $r_{CN} = 1.17$	2149.7 (96), 417.4 (144), 120.8 (4 × 2)
GaNC	−94.931 06	$r_{GaN} = 1.97$; $r_{CN} = 1.19$	2023.0 (390), 388.2 (121), 39.4 (1 × 2)
GaCN	−94.928 98	$r_{GaC} = 2.12$; $r_{CN} = 1.17$	2147.0 (92), 339.3 (105), 111.6 (2 × 2)
InNC	−94.763 15	$r_{InN} = 2.14$; $r_{CN} = 1.19$	2030.4 (348), 341.0 (104), 6.0i (1 × 2)
InCN	−94.762 63	$r_{InC} = 2.28$; $r_{CN} = 1.17$	2142.6 (73), 301.4 (92), 108.9 (2 × 2)
TlNC	−144.762 72	$r_{TlN} = 2.38$; $r_{CN} = 1.19$	2036.5 (275), 289.3 (87), 25.0i (0 × 2)
TlCN	−144.765 10	$r_{TlC} = 2.48$; $r_{CN} = 1.18$	2131.5 (45), 265.0 (79), 76.9 (0 × 2)

[a] All products are linear molecules. [b] For the major stable isotope.

tracking with the 2051.4 and 2011.2 cm^{-1} C≡N stretches in Figures 1b and 2b. The other peaks in Figure 3, at 456.2 and 450.3 cm^{-1}, similarly track with the 2143.7 and 2097.3 cm^{-1} pair from the C≡N stretching region.

Ga + HCN. Figures 1c and 2c display spectra for reactions of Ga with $H^{12}CN$ and $H^{13}CN$, respectively, following deposition for 90 min. Two absorptions dominate each spectrum. In Figure 1c, the band at 2046.4 cm^{-1} decreases moderately on photolysis and annealing and has a ^{13}C counterpart at 2005.8 cm^{-1}. The carbon-13 shift is 40.6 cm^{-1}, which is similar to the carbon-13 shift for the aluminum product bands in this region of the spectrum.

The other band of significance is at 2137.8 cm^{-1} in Figure 1c. Although the omnipresent CO stretching vibration is near this absorption, this band is relatively clean and is shifted to the red from the CO peak on its shoulder at 2138.0 cm^{-1}. The absorption intensity increases by 25% on photolysis and decreases 5% on annealing. The absorption at 2091.7 cm^{-1} in Figure 2c tracks with this band, yielding an isotopic shift of 46.1 cm^{-1}, which is also similar to that of the aluminum product absorption in this spectral region.

In the far-IR region, a weak broad band was observed at 401 ± 2 cm^{-1} for the $H^{12}CN$ reaction.

In + HCN. As with the other group 13 metals, ablating indium in the presence of HCN produced two major new product bands in the C≡N region; these spectra are presented in Figures 1d and 2d. The higher frequency product absorption in Figure 1d, at 2132.4 cm^{-1}, increases more than 2-fold in intensity on photolysis and remains virtually unchanged on annealing. This band and its carbon-13 counterpart at 2086.7 cm^{-1} indicates that the photolysis process that follows ablation generates more of this product than ablation alone. The 45.7 cm^{-1} isotopic shift is also consistent with the other products in this region.

The other major band, at 2051.1 and 2009.9 cm^{-1} for $H^{12}CN$ and $H^{13}CN$, respectively, decreases significantly on photolysis and moderately on annealing. The concurrent increase in the higher frequency peak intensity suggests that broad-band photolysis of the matrix enables interconversion of the two products. Also, the isotopic separation of the lower band, 41.2 cm^{-1}, is similar to those of the other experiments presented here.

Far-IR absorptions were observed at 392 and 333 cm^{-1} in the $H^{12}CN$ experiments. The former band decreases on photolysis while the latter increases, thereby tracking these peaks with the 2051.1 and 2132.4 cm^{-1} bands, respectively.

Tl + HCN. Figures 1e and 2e, each representing spectra following 90 min deposition of laser-ablated Tl with HCN, contain two major bands each, but also a broad cluster of bands to the blue of CO. The nearby sharp absorption at 2125.7 cm^{-1} increases 30% on photolysis and has a carbon-13 shift of 45.3 cm^{-1}. The broad bands also shift by approximately this amount and may represent product clusters with C≡N bonding characteristics similar to that of the nearby sharp band. The other major product absorption in these spectra at 2047.7 cm^{-1} decreases in intensity following photolysis. A single broad band was observed in each of the far-IR experiments with $H^{12}CN$ and $H^{13}CN$ at 307 ± 2 and 302 ± 2 cm^{-1}, respectively.

B + HCN. Figures 1a and 2a represent spectra of boron−hydrogen cyanide reactions.[4] Although there are several other absorptions at lower frequencies, only the C≡N stretching region is presented for comparison with the other group 13 products. Note that, because the sample is natural boron, two isotopic counterparts are observed for each product. Eighty percent of the products contain ^{11}B with the remaining 20% containing ^{10}B. For the ^{11}B products, the carbon-13 isotopic shift for the upper band, 48.6 cm^{-1}, is close to that of the other products in this region, while the isotope shift for the lower band, 33.6 cm^{-1}, is noticeably smaller than those of the analogous products from the other experiments.

Calculations. DFT/BP86 calculations for all MCN and MNC species are presented in Table 2. Use of the effective core potential for Tl products saved a great deal of time at little cost to accuracy for the desired information. Although using the effective core potential did not save nearly as much time for the other products, the calculations were performed similarly for comparison. For all but the Tl products, the MNC configuration is slightly energetically favorable to the MCN isomer, and the C≡N bond length is longer for each isocyanide molecule than for the corresponding cyanide molecule. Also, M−N bonds are significantly shorter than M−C bonds. In terms of vibrational frequency, the C≡N stretch of the isocyanide compounds is calculated to be at least 95 cm^{-1} lower than the corresponding cyanide molecule. For Ga, In, and Tl, only the C≡N stretch is calculated to be above 400 cm^{-1} (i.e., in the spectral range of the experiment). A few calculations produced imaginary frequencies for the bending mode, but the C≡N frequencies are very accurate even in these cases, as will be shown.

Discussion

Product Identification. With the exception of boron, reactions of laser-ablated group 13 elements with hydrogen cyanide form only two types of products: cyanides and isocyanides. Only for B + HCN reactions are cyanide products retaining hydrogen formed and trapped.[4] Although Table 1 and the product spectra indicate that all MH diatomic products are formed,[23−26] none of the bands in the cyanide and isocyanide region shift in the deuterated experiments.

Based on the calculations in Table 2 and the previous boron results, C≡N stretching frequencies should be greater than 2100 cm^{-1} for cyanides and between 2000 and 2100 cm^{-1} for the isocyanides. Note that, for each element in these experiments, one prominent band fits the profile for the cyanide and the other prominent absorption fits the isocyanide profile, and these

TABLE 3: Observed and BP86 Calculated Vibrational Frequencies (cm^{-1}) for MCN Products

product	observed	calculated	scale factor[a]
$^{11}B^{12}CN$	2170.7	2177.2	0.997
$^{10}B^{12}CN$	2171.5	2177.7	0.997
$^{11}B^{13}CN$	2122.1	2127.7	0.997
$^{10}B^{13}CN$	2122.8	2128.3	0.997
$Al^{12}CN$	2143.7	2149.7	0.997
$Al^{13}CN$	2097.3	2102.7	0.997
$Ga^{12}CN$	2137.8	2147.0	0.996
$Ga^{13}CN$	2091.7	2100.1	0.996
$In^{12}CN$	2132.4	2142.6	0.995
$In^{13}CN$	2086.7	2096.0	0.996
$Tl^{12}CN$	2125.7	2131.5	0.997
$Tl^{13}CN$	2080.4	2085.4	0.998

[a] Observed frequency divided by calculated frequency.

identifications are presented in the last column of Table 1. For comparison with experiment, Tables 3 and 4 show that the BP86 calculations using effective core potentials for each group 13 atom output vibrational frequencies in very good agreement with both the cyanides and isocyanides. In a previous study of Be−HCN products, the BP86 functional proved to be superior for predicting observed frequencies than more sophisticated methods.[5] The use of the frozen core pseudopotential on the M atom arises because doing otherwise would prohibit the TlCN and TlNC calculations from converging and because using the same method for all systems allows for better comparison.

Schaefer and co-workers predicted harmonic frequencies for natural isotopes of AlCN and AlNC using SCF calculations with the TZ2P + f basis sets and obtained results similar to our own.[13] The C≡N stretching frequency increases from 2290 cm^{-1} for AlNC to 2479 cm^{-1} for AlCN, results which are higher than we observed but are probably reasonably close to the actual harmonic frequencies. For AlNC, the Al−N stretching vibrational frequency calculation at 584 cm^{-1} is similarly to the blue of the Al−C stretching frequency of AlCN at 472 cm^{-1}.

For these calculations as well as the BP86 results, all of the products are calculated to be linear, but the bond lengths show definite trends. First, the M−N and M−C bonds increase with increasing size of M, as expected. A more notable trend is that C≡N bond lengths are shorter for each MCN molecule than for the corresponding MNC molecule. Accordingly, the M−C bonds are longer than the corresponding M−N bonds. This suggests that the cyanides have a full C≡N triple bond and M−C single bond, while the isocyanides have less triple bond character in the C≡N bond and a trace of double bond character in the M−N bond. That the C≡N stretching frequencies for the MCN molecules appear approximately 90 cm^{-1} higher in energy than for MNC confirms this hypothesis.

For the isocyanide C≡N stretching modes, the frequency is nearly independent of the M atom. The mean isocyanide frequencies are 2050.4 cm^{-1} for $MN^{12}C$ and 2011.0 cm^{-1} for $MN^{13}C$, with standard deviations of 3.5 and 6.4 cm^{-1}, respectively. Because the BNC frequencies are higher than expected due to Fermi resonance, they tend to account for much of the deviation, especially for $^{10}BN^{13}C$, which is affected more by the Fermi resonance than other isotopic molecules.[4,28] If one excludes BNC from the average of the isocyanide frequencies, the results are 2049.1 and 2008.3 cm^{-1} with standard deviations of 2.5 and 2.6 cm^{-1}. Also, there is no noticeable decrease or increase of this frequency with respect to atomic mass. Although the BP86 calculations predict a weak positive correlation between isocyanide C≡N frequency and atomic mass, the spectra show that, in the absence of Fermi resonance, the C≡N stretching frequency is nearly independent of the group 13 metal atom.

TABLE 4: Observed and BP86 Calculated Vibrational Frequencies (cm^{-1}) for MNC Products

product	observed	calculated	scale factor[a]
$^{11}B^{12}NC$	2055.2	2010.5	1.022
$^{10}B^{12}NC$	2068.0	2011.4	1.028
$^{11}B^{13}NC$	2021.6	1973.8	1.024
$^{10}B^{13}NC$	2039.6	1974.9	1.033
$Al^{12}NC$	2051.4	2024.4	1.013
$Al^{13}NC$	2011.2	1984.0	1.014
$Ga^{12}NC$	2046.4	2023.0	1.012
$Ga^{13}NC$	2005.8	1982.3	1.012
$In^{12}NC$	2051.1	2030.4	1.010
$In^{13}NC$	2009.9	1989.3	1.010
$Tl^{12}NC$	2047.7	2036.5	1.006
$Tl^{13}NC$	2006.4	1995.0	1.006

[a] Observed frequency divided by calculated frequency.

TABLE 5: Experimental Frequencies (cm^{-1}), Isotope Shifts (cm^{-1}), and Isotopic Ratios for MCN and MNC Products

	^{12}C freq	^{13}C freq	^{13}C shift	isotopic ratio[a]
^{11}BCN	2170.7	2122.1	48.6	1.022 90
^{10}BCN	2171.5	2122.8	48.7	1.022 94
AlCN	2143.7	2097.3	46.4	1.022 12
GaCN	2137.8	2091.7	46.1	1.022 04
InCN	2132.4	2086.7	45.7	1.021 90
TlCN	2125.7	2080.4	45.3	1.021 77
^{11}BNC	2055.2	2021.6	33.6	1.016 62
^{10}BNC	2068.0	2039.6	28.4	1.013 92
AlNC	2051.4	2011.2	40.2	1.019 99
GaNC	2046.4	2005.8	40.6	1.020 24
InNC	2051.1	2009.9	41.2	1.020 50
TlNC	2047.7	2006.4	41.3	1.020 58

[a] Carbon-12 frequency divided by carbon-13 frequency.

By contrast, the spectra of the cyanide molecules exhibit a definite negative correlation between frequency and atomic mass. Unlike in BNC, for BCN there is no Fermi resonance, but the C≡N stretching frequencies are much higher than for the metal cyanides. As the mass of the M atom is increased, this frequency decreases until it approaches a seemingly asymptotic value of about 2120 cm^{-1} for the $H^{12}CN$ experiments and about 2075 cm^{-1} for the $H^{13}CN$ experiments. The BP86 calculations also show this trend and predict MCN frequencies with excellent accuracy.

Although the absolute frequency shifts toward the red with increasing mass of M in MCN products, the carbon-13 shift is nearly the same for each species. Table 5 presents the isotopic data for both MCN and MNC products, as well as the carbon isotopic ratio. While the isotopic shift is greatest for boron and decreases with the mass of the M atom, this dependence is weak. The average of all of these carbon-13 shifts is 46.4 cm^{-1} with a standard deviation of only 1.3 cm^{-1}. The isotopic ratio, ν_{C-12}/ν_{C-13}, also decreases a small amount upon increasing atomic mass of M and averages 1.0222 with a standard deviation of 0.0004.

Unlike for MCN, the carbon-13 shift of MNC species increases slightly with increasing atomic mass, as Table 5 clearly shows. This trend is even weaker if BNC is excluded. For the other four products, the average isotopic shift is 40.8 cm^{-1} with a standard deviation of only 0.5 cm^{-1} while the average carbon isotopic ratio, 1.0203, has a standard deviation of 0.0003. Comparing the cyanides and isocyanides then, the carbon-13 shift in cyanides is, on average, 5−6 cm^{-1} larger than those in isocyanides if factors such as Fermi resonance are not considered.

For the observed far-IR bands, the calculations are in reasonable agreement with experiment. The 401 cm^{-1} band in the Ga + $H^{12}CN$ experiment is the Ga−N stretching absorption

calculated at 388 cm^{-1} (versus 339 cm^{-1} for the Ga−C mode of GaCN). The 392 and 333 cm^{-1} bands are similarly due to InNC and InCN, respectively, and the tracking with the C≡N stretching modes is definitive. TlNC has bands calculated at 289 and 284 cm^{-1} for the Tl−N mode for $TlN^{12}C$ and $TlN^{13}C$, respectively, and these agree well with the observed 307 and 302 cm^{-1} peaks.

One further trend among these products is worth noting. According to Table 2, the isocyanide products are, in general, lower in energy than their cyanide counterparts. This has been determined at higher levels of theory for BCN/BNC and AlCN/AlNC.[13,28] This energy difference is largest for the boron products and becomes smaller with increasing atomic mass until the situation is reversed for thallium, where TlCN is lower than TlNC, at the DFT/BP86 level of theory.

Reaction Mechanisms. For reactions of Be and B with HCN, the presence of cyanides with hydrogen atoms indicated that insertion into the C−H bond potentially followed by rearrangement was a major reaction pathway.[4,5] For the heavier group 13 elements, this mechanism may occur, followed by loss of the H atom:

$$M^* + HCN \rightarrow [HMCN]^* \rightarrow MCN/MNC + H \qquad (1)$$

In reactions of Be with HCN, production of BeNC dominated generation of BeCN on deposition. Broad-band photolysis of the matrix afterward, however, sharply increased the intensity of the BeCN bands, while the BeNC absorptions declined accordingly. The photolysis apparently equilibrated the two isomers, indicating that the formation of BeNC was initially dynamically favored in the deposition. For this reason, an alternate mechanism was proposed in which the Be atom approached HCN from the nitrogen and displaced the hydrogen as in a S_N2 reaction. For Ga, Tl, and especially In, the growth of the cyanide band on photolysis corresponds to a large decrease in the isocyanide band, as in the Be reactions. Accordingly, the following mechanism may be the major process for the reaction of these metals with HCN:

$$M^* + NCH \rightarrow [MNCH]^{\ddagger} \qquad (2)$$

$$[MNCH]^{\ddagger} \rightarrow MNC + H \qquad (3)$$

In the aluminum spectra, both the cyanide and isocyanide peaks grow on photolysis, with the isocyanide growth much larger. No clearly dominant mechanism seems to exist for the Al−HCN system, but both reactions presented above may play a role in product formation. The large growth of the AlNC peak on photolysis may indicate that, because AlNC is of lower energy than AlCN, the equilibration process may, in fact, proceed counter to that from the Ga, In, and Tl systems. In the B−HCN experiments, BNC bands grew a great deal on photolysis while BCN bands similarly decreased in intensity. This indicates that the Al−HCN system is more like the boron reactions than those of the heavier group 13 elements.

Comparison with Alkaline Earth Compounds. Analogous reactions involving group 2 metal atoms and hydrogen cyanide have been reported.[6] The main products are similar, in that MNC is the major product and no products contain hydrogen in the heaviest four elements of the group. Carbon-13 isotopic shifts are very nearly 40.0 cm^{-1} for all elements of both groups, with the exception of BNC. Nevertheless, although the alkaline earth elements have but one fewer electron in their valence shell, their reactions with HCN yield product spectra with significant differences from their group 13 counterparts. For example, while the frequency of MNC is fairly constant for all these elements, it decreases with increasing mass of M for the group 2 metals.

The most striking difference between the two systems is the lack of observation of MCN in the group 2 case, whereas in the group 13 product spectra, MCN was clearly present for all elements. For the alkaline earth cyanides, MNC was calculated to be the more stable isomer for all metals, but by only a few kcal mol^{-1}, and the barrier to interconversion was also small. The explanation for this is the dominance of a mechanism similar to the one presented earlier, in which the M atom attacks the N atom, ejects the H atom, and is trapped prior to any rearrangement to the MCN isomer. If this were the case for all the group 13 atom reactions, however, no MCN would be observed in these spectra, either. The energy difference between MCN and MNC was calculated to be 1.5 kcal mol^{-1} for magnesium[29] and 5.5 kcal mol^{-1} for aluminum,[13] indicating that the interconversion process for the aluminum species is actually *less* favorable. Therefore, the aluminum reactions probably proceed at least partially via the insertion reaction 1. Dissociation of the intermediate would account for the observation of a reasonably strong AlH band in the aluminum experiments, while the MgH band in the magnesium experiments is barely noticeable. That is, Al inserts to form HAlCN, which in turn dissociates into AlH and CN. The comparison of aluminum and magnesium reactions indicates that the aluminum reactions occur via both the insertion and "S_N2" mechanisms.

Photolysis behavior of the heavier group 13 cyanides and isocyanides suggests that the "S_N2" mechanism dominates, and only through rearrangement would MCN be formed. According to DFT calculations, the difference in energy between MNC and MCN becomes very small with Ga, In, and Tl. Bauschlicher et al. do not in their calculations observe this trend for the alkaline earth species, instead predicting little change in energy difference for magnesium, calcium, and barium cyanides and isocyanides.[29] For this reason, the observation of MCN for the heavier group 13 elements may simply be due to a lower isomerization barrier.

It is important to note that the calculated infrared intensities for the C−N stretching absorptions for the group 13 cyanides are somewhat larger than those of group 2. From this information alone, then, one could surmise that the lack of observation of MCN in the latter case owes to the low oscillator strength of the absorption band. However, the Mg−C stretching mode of MgCN is calculated to be comparable in intensity to the M−N or M−C modes of MgNC, AlCN, and AlNC. In the group 2 study, we conclude that the ratio [MgNC/MgCN] is very high because we would otherwise observe a Mg−C band. Because the Al−C band of AlCN and Al−N band of AlNC are of comparable intensity, it is likely that the two products are of comparable concentration in the matrix. Group 13 element reactions with HCN make significant amounts of MCN, whereas group 2 reactions do not.

Conclusions

In reactions of laser-ablated group 13 atoms with HCN, the major products are MNC and MCN. Except for the boron experiments, no new products containing hydrogen are formed. Cyanides are characterized by C≡N stretching frequencies between 2125 and 2175 cm^{-1}, for $M^{12}CN$, with a typical carbon-13 shift of approximately 45 cm^{-1}. The frequency of MCN is inversely related to the atomic mass of M. Isocyanides are characterized by C≡N stretching frequencies in a narrow range between 2045 and 2055 cm^{-1}, except for BNC, which is perturbed by Fermi resonance. The carbon-13 shift of MNC

products is less than that of MCN and is, on average, 40.8 cm^{-1} if BNC is excluded. Unlike the MCN case, the frequency of the C≡N stretch for MNC is in no obvious way related to the atomic mass of M.

As with Be + HCN reactions,[5] DFT/BP86 calculations work effectively for predicting C≡N vibrational frequencies, even when using a frozen core approximation for the M atom. These calculations show that the C≡N bonds in MCN are shorter than in MNC, while the M−C bonds are longer than the M−N bonds. Along with the bond length calculations, the fact that the cyanide frequencies are on the order of 100 cm^{-1} higher in energy than the isocyanide frequencies suggests that the C≡N bond in MCN has more "triple bond character" than in MNC. Similarly, the higher frequency of M−N absorptions in MNC indicates more metal "double bond character" than in MCN.

The calculations also indicate that MNC is in general more energetically stable than MCN, but this energy difference decreases with increasing atomic mass until the cyanide molecule is actually a bit more stable for the thallium products. For Ga, In, and Tl, the energy difference between the two isomers is quite small, and in these experiments, the cyanide product peak grows significantly on broad-band photolysis at the expense of the isocyanide peak. This interconversion is most likely an equilibration between the two isomers and indicates that, in the ablation/deposition process, the isocyanide product is formed disproportionately. A mechanism in which M approaches the N atom and ejects the H atom, akin to a S_N2 reaction, may explain the product spectra and is consistent with results from previously studied alkaline earth−hydrogen cyanide reactions.[5,6] Because of the absence of hydrogen products, it is possible that aluminum reactions follow this mechanism, but it is likely that, similar to the boron reactions, insertion into the C−H bond plays a role in product formation as well.

Although there are many similarities between the reactions of group 2 and group 13 elements with HCN, only in the latter case are significant amounts of MCN produced. For aluminum, this in all likelihood results because insertion plays a role, where it generally does not for the alkaline earth metals. For gallium, indium, and thallium, the relatively small energy difference between MCN and MNC suggests that interconversion between these two isomers is facile, which is apparently not the case with the corresponding group 2 species.

Acknowledgment. This work was supported by the Air Force Office of Scientific Research. Calculations were performed on the University of Virginia SP2 machine. Cambridge Isotope Laboratories kindly provided the $K^{13}CN$ sample.

References and Notes

(1) Hassanzadeh, P.; Hannachi, Y.; Andrews, L. *J. Phys. Chem.* **1993**, *97*, 6418.

(2) Andrews, L.; Hassanzadeh, P.; Martin, J. M. L.; Taylor, P. R. *J. Phys. Chem.* **1993**, *97*, 5839.

(3) Burkholder, T. R.; Andrews, L. *J. Phys. Chem.* **1992**, *96*, 10195.

(4) Lanzisera, D. V.; Andrews, L.; Taylor, P. R. *J. Phys. Chem. A* **1997**, *101*, 7134.

(5) Lanzisera, D. V.; Andrews, L. *J. Am. Chem. Soc.* **1997**, *119*, 6392.

(6) Lanzisera, D. V.; Andrews, L. *J. Phys. Chem. A* **1997**, *101*, 9666.

(7) Oxtoby, D. W.; Nachtrieb, N. H. *Principles of Modern Chemistry*; CBS College Publishing: Philadelphia, 1986.

(8) Thompson, C. A.; Andrews, L. *J. Am. Chem. Soc.* **1995**, *117*, 10125.

(9) Thompson, C. A.; Andrews, L.; Martin, J. M. L.; El-Yazal, J. *J. Phys. Chem.* **1995**, *99*, 13839.

(10) Lanzisera, D. V.; Andrews, L. *J. Phys. Chem. A* **1997**, *101*, 5082.

(11) Guélin, M.; Cernicharo, J.; Kahane, C.; Gomez-Gonzalez, J. *Astron. Astrophys.* **1986**, *157*, L17.

(12) Cernicharo, J.; Guélin, M. *Astron. Astrophys.* **1987**, *183*, L10.

(13) Ma, B.; Yamaguchi, Y.; Schaefer, H. F. *Mol. Phys.* **1995**, *86*, 1331.

(14) Bohn, R. B.; Andrews, L. *J. Phys. Chem.* **1989**, *93*, 3974.

(15) Gaussian 94, Revision B.1: Frisch, M. J.; Trucks, G. W.; Schlegel, H. B.; Gill, P. M. W.; Johnson, B. G.; Robb, M. A.; Cheeseman, J. R.; Keith, T.; Petersson, G. A.; Montgomery, J. A.; Raghavachari, K.; Al-Laham, M. A.; Zakrzewski, V. G.; Ortiz, J. V.; Foresman, J. B.; Cioslowski, J.; Stefanov, B. B.; Nanayakkara, A.; Challacombe, M.; Peng, C. Y.; Ayala, P. Y.; Chen, W.; Wong, M. W.; Andres, J. L.; Replogle, E. S.; Gomperts, R.; Martin, R. L.; Fox, D. J.; Binkley, J. S.; Defrees, D. J.; Baker, J.; Stewart, J. P.; Head-Gordon, M.; Gonzalez, C.; Pople, J. A. Gaussian, Inc., Pittsburgh, PA, 1995.

(16) Becke, A. D. *Phys. Rev. A* **1988**, *38*, 3098.

(17) Perdew, J. P. *Phys. Rev. B* **1986**, *33*, 8822.

(18) McLean, A. D.; Chandler, G. S. *J. Chem. Phys.* **1980**, *72*, 5639.

(19) Krishnan, R.; Binkley, J. S.; Seeger, R.; Pople, J. A. *J. Chem. Phys.* **1980**, *72*, 650.

(20) Hay, P. J.; Wadt, W. R. *J. Chem. Phys.* **1985**, *82*, 270.

(21) Wadt, W. R.; Hay, P. J. *J. Chem. Phys.* **1985**, *82*, 284.

(22) Hay, P. J.; Wadt, W. R. *J. Chem. Phys.* **1985**, *82*, 299.

(23) Chertihin, G. V.; Andrews, L. *J. Phys. Chem.* **1993**, *97*, 10295.

(24) Pullumbi, P.; Mijoule, C.; Manceron, L.; Bouteiller, Y. *Chem. Phys.* **1994**, *185*, 13.

(25) Pullumbi, P.; Bouteiller, Y.; Manceron, L.; Mijoule, C. *Chem. Phys.* **1994**, *185*, 25.

(26) Huber, K. P.; Herzberg, G. *Molecular Spectra and Molecular Structure*; Van Nostrand Reinhold: New York, 1979.

(27) Chertihin, G. V.; Andrews, L.; Taylor, P. R. *J. Am. Chem. Soc.* **1994**, *116*, 3513.

(28) Martin, J. M. L.; Taylor, P. R. *J. Phys. Chem.* **1994**, *98*, 6105.

(29) Bauschlicher, C. W., Jr.; Langhoff, S. R.; Partridge, H. *Chem. Phys. Lett.* **1985**, *115*, 124.